BER Improvement Effect of Optical Delay Insertion in ROF Ubiquitous Antenna Architecture for Wireless CDMA System

Hideaki Ohtsuki, Katsutoshi Tsukamoto, *Member, IEEE*, and Shozo Komaki, *Senior Member, IEEE*

***Abstract*—This paper proposes an application of optical delay insertion to a radio-on-fiber ubiquitous antenna architecture for the wireless code-division multiple-access system. The proposed system separates each component of independent signals passing through the multipath in radio and optical links even though a mobile terminal exists anywhere in the service area, so the macrodiversity effect is obtained all over the area. As a result, bit error rate performance is improved by setting up the delay time difference between each optical link and the number of taps in the RAKE receiver appropriately.**

***Index Terms*—Delay insertion, macrodiversity, radio-on-fiber (ROF), RAKE reception, ubiquitous antenna system.**

I. Introduction

RECENTLY, the demand for high-speed and high-capacity multimedia services in wireless communication systems has been growing rapidly. Thus, the microcellular system, which consists of many small cells, has attracted attention as an effective method for attaining high-speed and high-capacity communication by improving frequency utilization efficiency. However, the microcellular system has some problems, such as the large investment required in many radio base-station (RBS) facilities and the necessity for complicated channel control techniques among RBSs for spectral delivery and the handoff/over procedure.

A radio-on-fiber (ROF) system that interconnects many RBSs to a microcell control station (MCS) has been proposed to solve these problems [1]–[4]. We have previously proposed an ROF ubiquitous antenna architecture, which is composed of multiple microcell RBSs deployed over the service area [5]. Fig. 1 illustrates the configuration of an ROF ubiquitous antenna system where an RBS is only equipped with electric-to-optic (E/O) and optic-to-electric (O/E) converters, and all of the complicated functions such as RF modulation, demodulation, channel control and so on, are performed at an MCS. The MCS can deliver different radio signals simultaneously to different places and can gather many radio signals simultaneously from many radio cells. Therefore, it can enable software radio networks that realize universal capability and flexibility for various types of air interface. Another important effect is macrodiversity capability, because an MCS can receive not only any radio signal on the multipath in a small cell but also some signals on the photonic multipath which has its mutual independence [6].

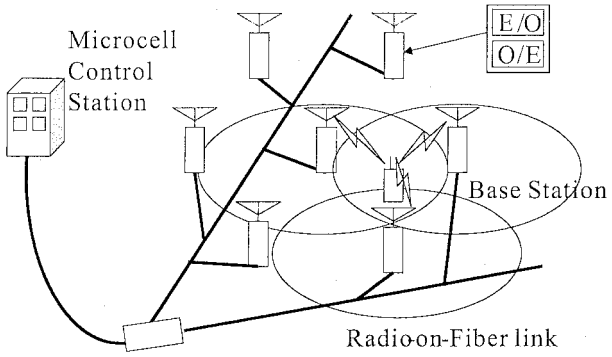

Fig. 1. Configuration of ROF ubiquitous antenna system.

When we construct an ROF ubiquitous antenna architecture, the single star-type configuration is a large investment. In order to reduce the required investment for an ROF ubiquitous antenna architecture, a bus-type or a passive double star (PDS) type configuration is preferable. However, a drawback of these configurations is that some independently faded radio signals are gathered in a single fiber and are photodetected at one receiver of the MCS. Therefore, we must distinguish each of them to obtain macrodiversity effect. As is well known, a code-division multiple-access (CDMA) system can separate each component received from multiple paths by using RAKE reception [7]. There are many studies on CDMA techniques in the world. CDMA techniques with macrodiversity have been studied [8], [9]. Reference [8] has analyzed the uplink capacity and the transmission power, taking the macrodiversity effect into account the DS-CDMA system. Reference [9] has experimentally investigated the suppression of interference from an adjoining cell by using CDMA in an ROF system. These works have assumed a single star-type topology. On the other hand, we have focused an ROF ubiquitous antenna architecture of a PDS-type topology in the wireless CDMA system [10]. In that paper, we analyzed the transmission power reduction effect for an ROF ubiquitous antenna architecture of a PDS-type topology in the wireless CDMA system. In this topology, an MCS receives signals transmitted from different RBSs at a same chip timing. So the RAKE receiver cannot distinguish them. These signals pass through the different radio links, which have a different propagation characteristic.

Manuscript received April 27, 2003; revised August 11, 2003. This paper was supported in part by the Japan Society for the Promotion of Science under Grants-in-Aid for Scientific Research (B) 14350202.

The authors are with the Department of Communications Engineering, Graduate School of Engineering, Osaka University, Suita, 565-0871 Osaka, Japan (e-mail address: otsuki@roms.comm.eng.osaka-u.ac.jp).

Digital Object Identifier 10.1109/JLT.2003.821713

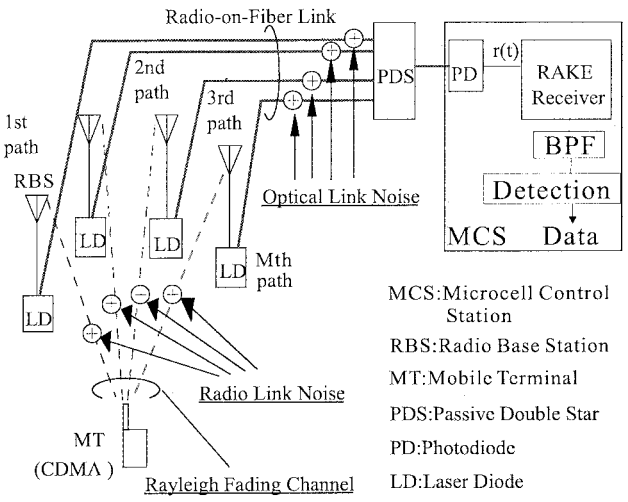

Fig. 2. System model.

Therefore these signals interfere with each other. Consequently the bit error rate (BER) performance becomes worse. In order to solve this problem, we propose the application of the optical delay insertion. So by setting up the delay time difference in optical link appropriately, an MCS will not receive signals transmitted from different RBSs at same chip timing even though a mobile terminal (MT) exists anywhere in the service area. Therefore the BER performance improves all over the service area.

In this paper, we propose the application of optical delay insertion to an ROF ubiquitous antenna architecture for the wireless CDMA system. We theoretically investigate the improvement of BER performance in the proposed system.

The rest of this paper is organized as follows. In Section II, we describe an ROF ubiquitous antenna architecture in the wireless CDMA system, followed by analysis results of BER improvement effect of the optical delay insertion in Section III. Concluding remarks are given in Section IV.

II. ROF Ubiquitous Antenna System

A. System Description

Fig. 2 illustrates the system model of an ROF ubiquitous antenna architecture for the wireless CDMA system. A direct-sequence (DS)-CDMA radio signal from an MT is received at M RBSs. At each RBS, received DS-CDMA radio signals are converted into an optical intensity-modulated (IM) signal by modulating the laser diode directly, and are then transmitted to an MCS through the optical fiber. The IM signals transmitted from each RBS are gathered at a star coupler in the PDS link and received at the MCS. At the MCS, the received IM signals are converted to electric signals at the photodiode. Next, the RAKE receiver detects a desired signal from among many signals passing through the multipath on radio and optical links. We assume cellular phone system, Intelligent Transport System (ITS) [9], and so forth. So we assumed a flat Rayleigh fading channel in the radio link and an additive white Gaussian noise channel in the optical link. Path loss in radio link L_r is calculated using the following equation:

$$L_r = d^{\alpha} \tag{1}$$

where d is the distance between RBS and MT and α is the path-loss exponent. We assume that $\alpha = 4$ [11].

B. Received SNR and BER Analysis

In this section, we derive the average BER in proposed system. First, we derive the signal-to-noise ratio (SNR) of the output of each tap of RAKE receiver. When there are no interfering MTs, the input of the RAKE receiver after bandpass filtering $r(t)$ is derived as

$$r(t) = \sum_{i=1}^{M} \frac{s(t-\tau_i)R_i}{\sqrt{Lr_i Lo_i}} + \sum_{i=1}^{M} \frac{n_{ri}(t)}{\sqrt{Lo_i}} + n_o(t) \tag{2}$$

where $s(t-\tau_i)$ is the CDMA signal transmitted through the ith path from the MT, τ_i is the time delay of the ith path, which has lengths different from each other, $n_{ri}(t)$ is the noise in the ith radio link, $n_o(t)$ is the total noise in the optical link, L_{r_i} is the path loss in the radio link of the ith path, and L_{o_i} is the path loss in the optical link of the ith path. Assuming a flat Rayleigh fading channel in each radio link, R_i is the Rayleigh distributed gain of the ith path. The probability distribution of R_i, $p_R(R_i)$, is given by [7]

$$p_R(R_i) = 2R_i \exp\left\{-{R_i}^2\right\} \qquad (i = 1 \sim M,\ R_i \geq 0) \tag{3}$$

where the mean square of R_i $\langle {R_i}^2 \rangle = 1$. We assume that each value of R_i is statistically independent.

Assuming that the RAKE receiver has M outputs corresponding to M macro multiple paths (M antenna diversity), the SNR of the mth tap output γ_m without any interference from other MTs is derived as

$$\gamma_m = \frac{\frac{S{R_m}^2}{Lr_m Lo_m}}{\left\{ N_o + \sum_{i=1}^{M} \frac{N_r}{Lo_i} + \sum_{\substack{i=1 \\ i \neq m}}^{M} \frac{S{R_i}^2}{Lr_i Lo_i} \right\}^{\frac{1}{K}}} \ (m = 1, 2, \ldots, M) \tag{4}$$

where S is the transmitted power of the MT, K is the process gain, N_r is the power of the noise in spreaded band in each radio link, and N_o is the total power of the noise in spreaded band in the optical link. Here the average SNR in the radio link of the ith path Γ_{r_i} and the average SNR in the optical link of the ith path Γ_{o_i} are, respectively, derived as

$$\Gamma r_i = \frac{S}{Lr_i N_r} \tag{5}$$

$$\Gamma o_i = \frac{S}{Lr_i Lo_i N_o}. \tag{6}$$

X_i is defined as

$$X_i = {R_i}^2 (i = 1 \sim M). \tag{7}$$

X_i is a random variable with a probability density function (pdf) of

$$p_{X_i}(X_i) = \exp\{-X_i\} \quad (i = 1 \sim M) \quad (X_i \geq 0). \tag{8}$$

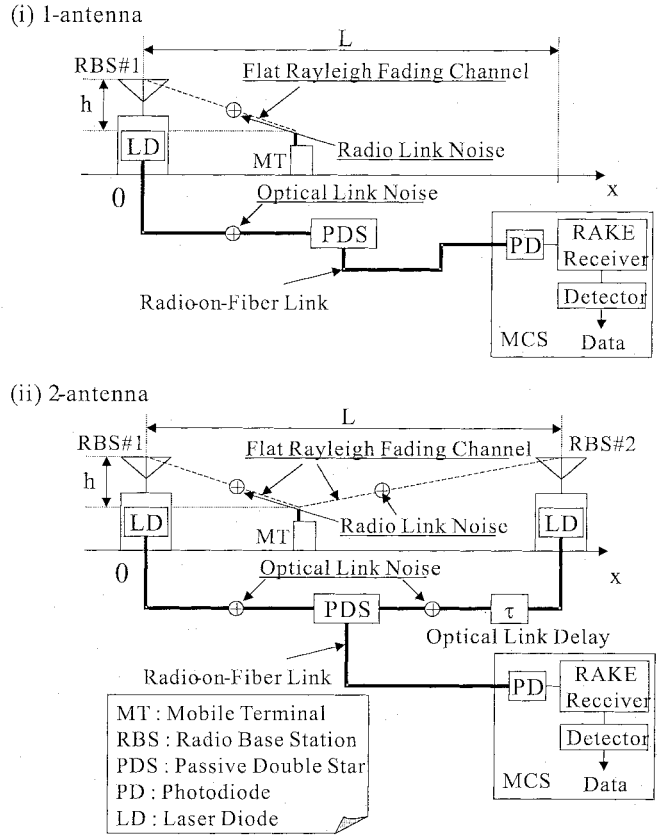

Fig. 3. Arrangement of RBSs.

Therefore, (4) is rewritten as

$$\gamma_m = \frac{K\Gamma o_m X_m}{1+\sum_{i=1}^{M}\frac{\Gamma o_i}{\Gamma r_i}+\sum_{\substack{i=1\\ i\neq m}}^{M}\Gamma o_i X_i}. \tag{9}$$

Next, we derive the pdf of γ, which is SNR at the output of the RAKE receiver. Because each value of X_i is statistically independent, $p_{X_1\cdots X_M}(X_1, X_2, \ldots, X_M)$ is written as [12]

$$\begin{aligned} p_{X_1\cdots X_M}(X_1, X_2, \ldots, X_M) &= \prod_{i=0}^{M} p_{X_i}(X_i) \\ &= \exp\left\{-(X_1 + X_2 + \cdots + X_M)\right\}. \end{aligned} \tag{10}$$

The joint pdf of γ_m ($m = 1 \sim M$) is written as [12]

$$\begin{aligned} &p_{\gamma_1\cdots\gamma_M}(\gamma_1, \gamma_2, \ldots, \gamma_M) \\ &\quad = \frac{1}{|J(X_1, X_2, \ldots, X_M)|} p_{X_1\cdots X_M}(X_1, X_2, \ldots, X_M) \end{aligned} \tag{11}$$

where $J(X_1, X_2, \ldots, X_M)$ is the Jacobian of (9) ($m = 1 \sim M$) and is written as [12]

$$J(X_1, X_2, \ldots, X_M) = \begin{vmatrix} \frac{\partial\gamma_1}{\partial X_1} & \frac{\partial\gamma_1}{\partial X_2} & \cdots & \frac{\partial\gamma_1}{\partial X_M} \\ \frac{\partial\gamma_2}{\partial X_1} & \frac{\partial\gamma_2}{\partial X_2} & \cdots & \frac{\partial\gamma_2}{\partial X_M} \\ \vdots & \vdots & \ddots & \vdots \\ \frac{\partial\gamma_M}{\partial X_1} & \frac{\partial\gamma_M}{\partial X_2} & \cdots & \frac{\partial\gamma_M}{\partial X_M} \end{vmatrix}. \tag{12}$$

When the RAKE receiver performs maximum ratio combining with M-order diversity, the obtained SNR γ at the output of the RAKE receiver is written as [7]

$$\gamma = \sum_{m=1}^{M} \gamma_m. \tag{13}$$

By using (9)–(13), the pdf of the received SNR γ can be derived. In the case of $M = 2$, a joint pdf of γ_1 and γ_2, $p_{\gamma_1\gamma_2}(\gamma_1, \gamma_2)$ is derived as shown in (14) at the bottom of the next page, where N and Δ_2 are given by

$$N = 1 + \sum_{i=1}^{M} \frac{\Gamma o_i}{\Gamma r_i} \tag{15}$$

and

$$\Delta_2 = K^2 - \gamma_1\gamma_2. \tag{16}$$

Thus, the pdf of γ, $p(\gamma)$ is given by

$$p(\gamma) = \int_0^{\gamma} p_{\gamma_1\gamma_2}(\gamma_1, \gamma - \gamma_1) d\gamma_1. \tag{17}$$

The cumulative distribution function of the received SNR, $P(\gamma \leq \nu)$ is given by

$$P(\gamma \leq \nu) = \int_0^{\nu} p(\gamma) d\gamma. \tag{18}$$

In the case of $M = 3, 4, \ldots,$ $p(\gamma)$ and $P(\gamma \leq \nu)$ are derived similarly.

Finally, we derive the average BER P_e. Assuming binary phase-shift keying as a primary modulation format, BER $p_e(\gamma)$ is given by [7]

$$p_e(\gamma) = \frac{1}{2}\mathrm{erfc}(\sqrt{\gamma}). \tag{19}$$

The average BER P_e is derived by

$$P_e = \int_0^{\infty} p_e(\gamma) p(\gamma) d\gamma. \tag{20}$$

III. BER Improvement Effect of Optical Delay Insertion

In this section, we discuss the BER performance for the delay time difference between the received signals. Fig. 3 shows the arrangement of RBSs in this analysis. We analyze the one- and two-antenna models. In the two-antenna model, we assume that the received signal at RBS #2 is delayed for τ in the optical link compared with the received signal at RBS #1 and received at the MCS. Fig. 4 shows the configuration of the RAKE receiver. The received signal passes through the matched filter. The output of the matched filter passes through the transversal filter. The outputs of the transversal filter are weighted according to maximum ratio combining (MRC) at each tap and are summed. We define the synchronization tap as a tap at which the largest signal is synchronized. Table I shows the values of parameters used in the numerical calculation. Fig. 5 shows the relationship between the average BER and the delay time difference in the optical link. In the calculation, it is assumed that the location of MT is in

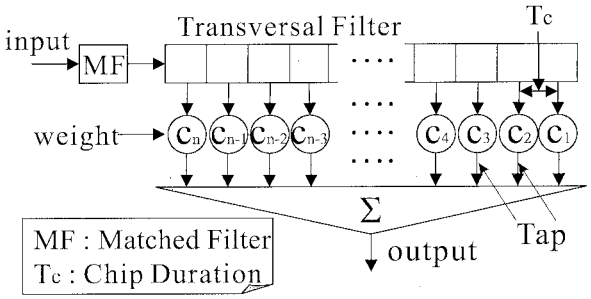

Fig. 4. Configuration of RAKE receiver.

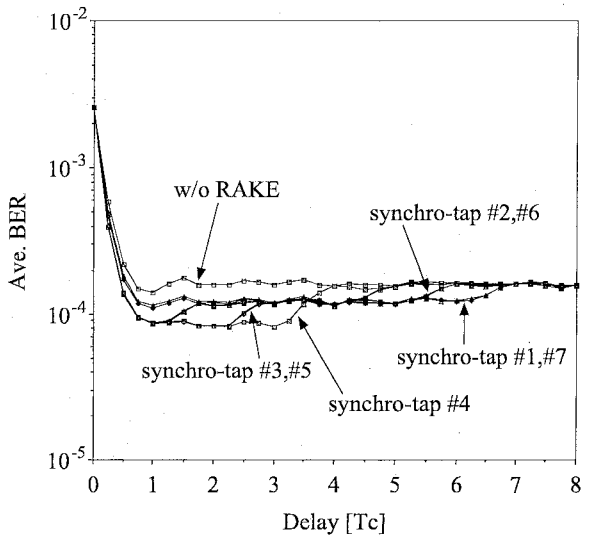

Fig. 5. Relationship between the average BER and the delay time difference in optical link. The position of the synchronization tap is changed.

TABLE I
PARAMETER USED IN NUMERICAL CALCULATION

Average SNR in Radio Link	Γr	0[dB]
Average SNR in Optical Link	Γo	20[dB]
Process Gain	K	100
Chip Rate		4[Mcps]
Chip Duration	T_c	0.25[μs]
Distance between RBSs	L	150[m]
Difference of height among RBS and MT	h	5[m]

the middle of two RBSs. We fix the number of taps in RAKE receiver to seven and vary the position of the synchronization tap. It is seen from Fig. 5 that the average BER becomes worse as the delay time difference in the optical link approaches zero. This is because when the delay time difference in the optical link is zero, the received signals at RBS#1 and RBS#2 are received at the MCS at same chip timing, so the RAKE receiver cannot distinguish each signal and combine. So both signals interfere with each other. On the other hand, when the delay time difference in the optical link is equal to or more than $1[T_c]$, the RAKE receiver can distinguish each signal and combine. So we can obtain the macrodiversity effect. When the delay time difference in the optical link is equal to or more than $1[T_c]$, the average BER has three level values. The average BER is the best value, when both signals from RBS#1 and RBS#2 are received and combined. The average BER is the middle value, when either signal from RBS#1 or RBS#2 is surely received but the other signal from the RBS#2 or the RBS#1 is sometimes received. This is because either signal from the RBS#1 or the RBS#2 is received at the synchronization tap; the other signal is received sometimes out of tap. The average BER is the worst value, when either signal from the RBS#1 or the RBS#2 is received but the other signal is received always out of tap. It is seen from Fig. 5 that when we set the position of the synchronization tap for four, the best BER performance can maintain for larger delay time difference in the optical link compared with others. So by setting the synchronization tap to the middle tap, the best BER performance can maintain for large delay time difference in the optical link. This is because the signal, which is not received at the synchronization tap, is received for larger delay time difference in the optical link.

Next, we think about the number of taps in the RAKE receiver. Fig. 6 shows the relationship between the average BER and the delay time difference in the optical link. In the calculation, it is assumed that the location of MT is the middle of two RBSs. We change the number of taps in the RAKE receiver and fix the position of the synchronization tap for the middle tap. It is seen from Fig. 6 that when the number of taps in the RAKE receiver is large, the best BER performance can maintain for large delay time difference in the optical link.

Fig. 7 shows the relationship between the average BER and the location of MT without RAKE reception. This relationship in one-antenna model is also shown. Figs. 8 and 9 show the relationship between the average BER and the location of MT in the case that the number of taps in the RAKE receiver is seven and nine, respectively. It is seen from these three figures that when the delay time difference in the optical link is $0[T_c]$, the average BER becomes worse as the location of MT approaches the middle. This is because the delay time difference in the radio link becomes zero around the middle of RBSs. Signals from the RBS#1 and the RBS#2 are received at the same chip timing. So the RAKE receiver cannot distinguish each signal and combine. Similarly, when the delay time difference in the optical link is

$$p_{\gamma_1\gamma_2}(\gamma_1,\gamma_2)=\begin{cases}\frac{N^2K^2(K+\gamma_1)(K+\gamma_2)}{\Gamma o_1\Gamma o_2\Delta_2^3}\cdot\exp\left\{-\frac{N(K+\gamma_1)(K+\gamma_2)}{\Delta_2}\left\{\frac{\gamma_1}{\Gamma o_1(K+\gamma_1)}+\frac{\gamma_2}{\Gamma o_2(K+\gamma_2)}\right\}\right\} & (\Delta_2>0)\\ 0 & (\Delta_2\le 0)\end{cases} \tag{14}$$

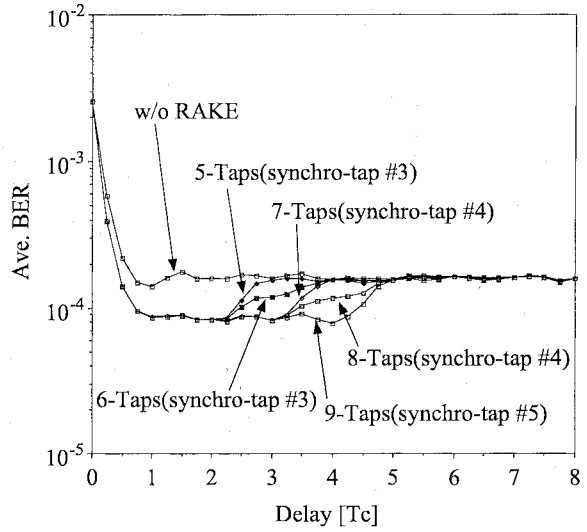

Fig. 6. Relationship between the average BER and the delay time difference in optical link. The number of taps of RAKE receiver is changed.

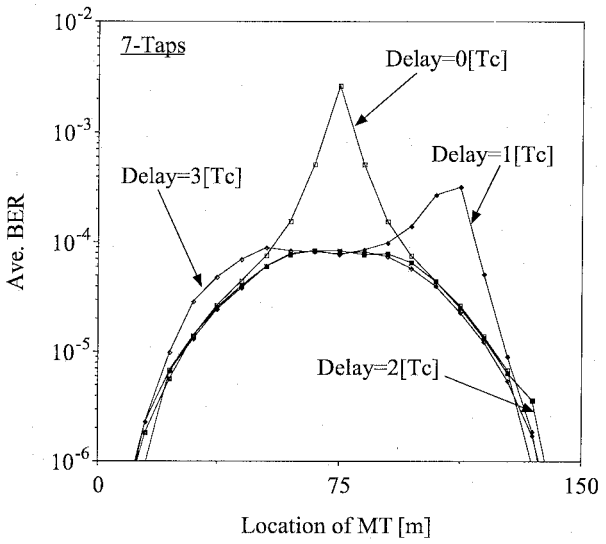

Fig. 8. Relationship between the average BER and location of MT (seven taps).

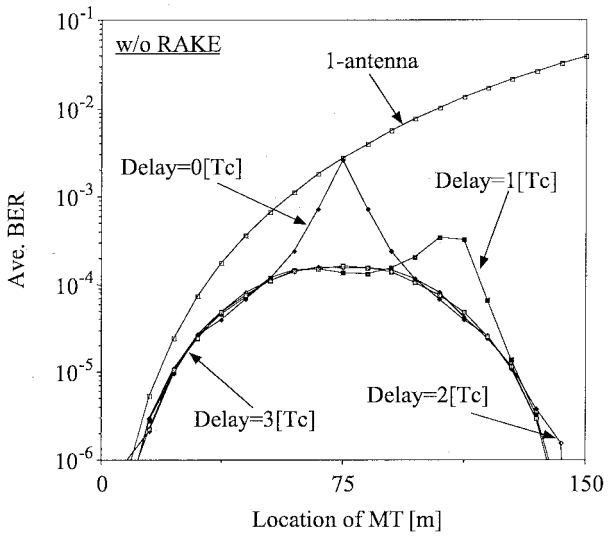

Fig. 7. Relationship between the average BER and location of MT (without RAKE).

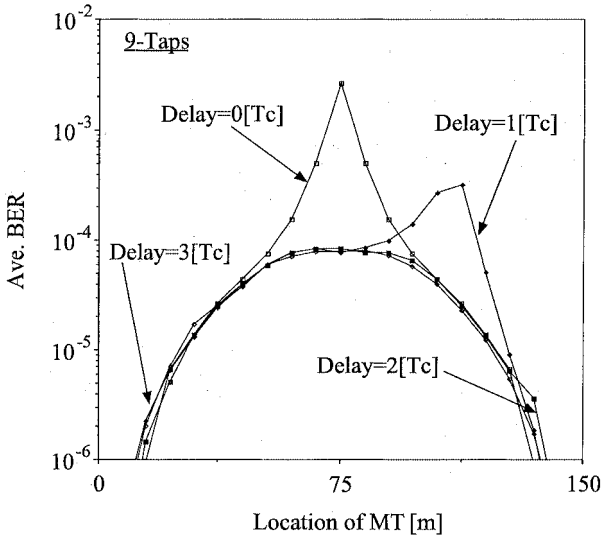

Fig. 9. Relationship between the average BER and location of MT (nine taps).

$1[T_c]$, the average BER becomes worse as the location of MT approaches 110[m]. This is because the delay time difference in the radio link plus the optical link also becomes zero. In addition, when the delay time difference in the optical link is $2[T_c]$, the average BER becomes a little worse as the location of MT approaches the RBS#2. This is because the delay time difference in the radio link plus the optical link also becomes zero but one of received signal is very larger than the other one. So BER performance does not become worse without diversity. On the other hand, when the delay time difference in the optical link is $3[T_c]$, the average BER does not become worse. This is because the delay time difference in the radio link plus the the optical link does not become zero. However, it is seen from Fig. 8 that when the delay time difference in the optical link is $3[T_c]$, the average BER becomes worse as the location of MT approaches the RBS#1. This is because the delay time difference in the radio link plus the optical link becomes large, so one of received signals from the RBS#1 and the RBS#2 arrives out of tap in the RAKE receiver. On the other hand, in Fig. 9, when the delay time difference in the optical link is $3[T_c]$, average BER does not become worse. This is because when the number of taps in the RAKE receiver becomes large, both signals arrive within tap in the RAKE receiver.

It is seen from these results that by setting up the delay time difference in the optical link and the number of taps in the RAKE receiver, our proposed system improves the BER performance all over the service area. So we expect that it can reduce required peak power by about 15 [dB] to achieve required BER [7], so it can downsize MTs.

IV. Conclusion

In this paper, we have proposed the application of the optical delay insertion in an ROF ubiquitous antenna architecture for the wireless CDMA system. In the proposed system, by setting

up the delay time difference in the optical link and the number of taps in the RAKE receiver appropriately, an MCS will not receive signals transmitted from different RBSs at the same chip timing even though an MT exists anywhere in the service area. Therefore, the BER performance improved all over the service area. For example, when the distance between RBSs is 150 [m], we can obtain the BER improvement all over the area by setting the number of taps to nine and the delay time difference in the optical link to $3[T_c]$. We also have analyzed the BER performance for the delay time difference in the optical link. From the results of theoretical examination, we have verified that by setting up the delay time difference, our proposed system improves the BER performance all over the service area compared with an ROF ubiquitous antenna architecture for the wireless CDMA without optical delay insertion.

REFERENCES

[1] "Application of RF and microwave subcarriers to optical fiber transmission in presence in recent and future broadband networks," *IEEE J. Select. Areas Commun.*, vol. 8, Sept. 1990.

[2] A. J. Cooper, "Fiber/radio for the provision of cordless/mobile telephony services in the access network," *Electron. Lett.*, vol. 26, no. 24, pp. 2054–2056, Nov. 1990.

[3] T. S. Chu and M. J. Gans, "Fiber optic microcellular radio," *IEEE Veh. Technol.*, pp. 339–344, May 1991.

[4] S. Komaki, K. Tsukamoto, M. Okada, and H. Harada, "Network considerations on fiber optic microcellular radio systems," *24th EuMC-WS*, vol. 1, pp. 46–51, Sept. 1994.

[5] K. Tsukamoto, Y. Kadota, M. Okada, and S. Komaki, "Macro diversity using photonic fed ubiquitous antenna architecture for road-to-vehicle communication," in *Proc. Wireless Personal Multimedia Communications '99*, Sep. 1999, pp. 468–473.

[6] Y. Park, S. Miyamoto, S. Komaki, and N. Morinaga, "The effect of co-channel interferences on intercell diversity in the optical microcell system," IEICE, SAT93–62, RCS93–68, 1993.

[7] J. G. Proakis, *Digital Commun.*, 4th ed: New York McGraw-Hill, Electrical Engineering Series, pp. 840–852.

[8] K. Ohno and F. Adachi, "Reverse-link capacity and transmit power in a power-controlled cellular DS-CDMA system," *IEICE Trans. Commun.*, vol. J79-B, no. 1, pp. 17–18, Jan. 1996.

[9] H. Harada, K. Sato, and M. Fujise, "A radio-on-fiber based millimete-wave road-vehicle by a code division mulitiplexing radio transmission scheme—Symmetry between uplink and downlink," in *Proc. ITST'2001*, Oct. 2001, pp. 47–52.

[10] H. Ohtsuki, K. Tsukamoto, and S. Komaki, "Transmission power reduction effect in wireless CDMA system employing ROF ubiquitous antenna architecture," in *Proc. MWP2002*, Oct. 2002, pp. 257–260.

[11] M. Hata, "Empirical formula for propagation loss in land mobile radio service," *IEEE Trans. Veh. Technol.*, vol. VT-29, pp. 317–325, Aug. 1980.

[12] A. Papoulis, *Probability, Randam Variables, and Stochastic Processes*, 3rd ed: New York McGraw-Hill, Electrical Engineering Series.

Hideaki Ohtsuki was born in Osaka, Japan, on June 8, 1976. He received the B.E. and M.E. degrees in communication engineering from Osaka University, Osaka, in 2000 and 2001, respectively, where he is currently pursuing the Ph.D. degree.

He is engaging in research on radio and optical communication systems.

Katsutoshi Tsukamoto (S'88–M'88) was born in Shiga, Japan, in October 7, 1959. He received the B.E., M.E., and Ph.D. degrees in communications engineering from Osaka University, Osaka, Japan, in 1982, 1984, and 1995, respectively.

He is currently an Associate Professor in the Department of Communications Engineering, Osaka University, engaging in research on radio and optical communication systems.

He is a member of the Institute of Television Engineers of Japan. He received the Paper Award from the Institute of Electronics and Information Communication Engineers of Japan in 1996.

Shozo Komaki (M'84–SM'94) was born in Osaka, Japan, in 1947. He received B.E., M.E., and Ph.D. degrees in electrical communication engineering from Osaka University, in 1970, 1972, and 1983 respectively.

In 1972, he joined NTT Radio Communication Laboratories, where he was engaged in repeater development for a 20-GHz digital radio system and 16-QAM and 256-QAM systems. In 1990, he joined the Faculty of Engineering, Osaka University, engaging in research on radio and optical communication systems. He is currently a Professor at Osaka University.

Dr. Komaki is a Fellow of the Institute of Electronics and Information Communication Engineers of Japan (IEICE) and the Institute of Television Engineers of Japan. He received the Paper Award and the Achievement Award from IEICE, Japan, in 1977 and 1994, respectively.